

PROCEEDINGS OF SPIE

[SPIDigitalLibrary.org/conference-proceedings-of-spie](https://spiedigitallibrary.org/conference-proceedings-of-spie)

Miniature illuminator for laser Doppler velocimeter assembled on micromachined silicon optical bench

Alexander Ksendzov, Richard D. Martin, Darius Modarress, Mory Gharib

Alexander Ksendzov, Richard D. Martin, Darius Modarress, Mory Gharib, "Miniature illuminator for laser Doppler velocimeter assembled on micromachined silicon optical bench," Proc. SPIE 3878, Miniaturized Systems with Micro-Optics and MEMS, (2 September 1999); doi: 10.1117/12.361273

SPIE.

Event: Symposium on Micromachining and Microfabrication, 1999, Santa Clara, CA, United States

Miniature Illuminator for Laser Doppler Velocimeter Assembled on Micromachined Silicon Optical Bench

A. Ksendzov^{a*}, R.D. Martin^b, D. Modarress^c, M. Gharib^c

(a) Jet propulsion Laboratory, California Institute of Technology, Pasadena, CA 91109

(b) W.L. Gore & Associates, Newark, DE 19713

(c) Dept. of Aeronautics, California Institute of Technology, Pasadena, CA 91125

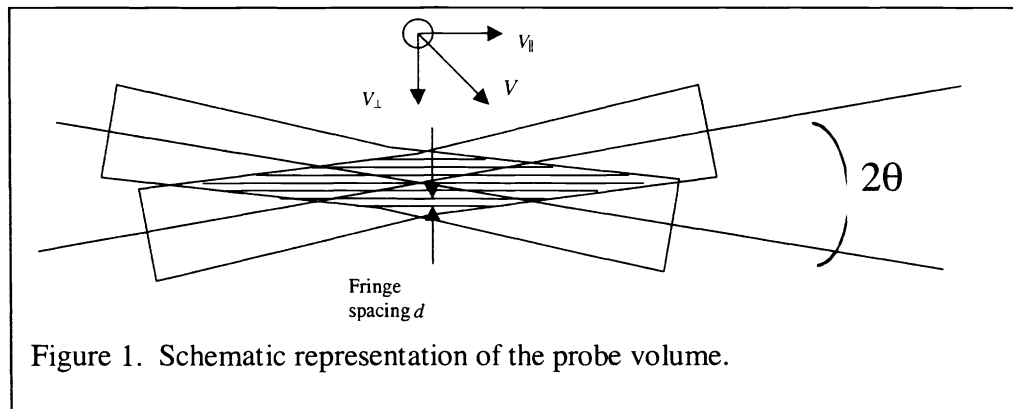
Keywords: Doppler velocimeter, anemometer, micromachined, silicon optical bench

ABSTRACT

We have built a miniature illuminator for Laser Doppler velocimeter on micromachined silicon optical bench utilizing a novel optical scheme. We used two intersecting coherent beams from the two opposing facets of semiconductor laser die to form a standing interference pattern needed for the particle detection and velocity measurement. Such devices are of interest to NASA for investigating wind patterns and dust loading on planets with atmosphere. They have been applied to problems where the liquid or gas flux must be characterized without disturbing the flow. In addition, the small probe volume makes possible local flow characterization and profiling. The device fabrication, and the results of the fringe characterization and velocity measurements are presented and discussed.

INTRODUCTION

The laser Doppler velocimeter can be used for remote contactless measurement of



velocity of objects moving through a transparent medium. The measurement utilizes two intersecting coherent light beams producing a standing fringe pattern, as illustrated in Figure 1.

* Correspondence: e-mail: alexander.ksendzov@jpl.nasa.gov

An object crossing the fringes gives rise to light scattering modulated in time with the frequency determined by the object velocity and the fringe spacing. The fringe spacing d is given by the following expression:

$$d = \lambda / (2 \sin \theta), \quad (1)$$

where λ is the wavelength of the light source, and 2θ is the angle between the crossing beams (see Fig. 1). Therefore the observed signal frequency f is

$$f = 2V_{\perp} \sin \theta / \lambda, \quad (2)$$

where V_{\perp} is the velocity component normal to the fringes.

The uses of such devices include contactless liquid and gas velocity measurements. In all applications the presence of light scatterers such as dust particles in air flow¹ or red blood cells travelling with blood stream² facilitates measurements. The possibility of achieving a small probe volume is a useful feature allowing for local velocity measurements needed for flow profiling as well as monitoring flow in small volumes. In addition, reducing the probe volume increases the intensity of the scattered light and facilitates detection of smaller particles.

Earlier approaches utilized light from one laser die facet and used a beamsplitter¹ or a grating³ to create two intersecting coherent beams. In our view, the use of coherent beams from two opposite laser die facets simplifies the device fabrication and alignment. Such scheme has been validated recently by Ito *et al*⁴ who fabricated a miniature integrated velocimeter as a planar structure less than 1 mm². The applications of the latter device however seem to be limited to objects placed very closely to the velocimeter due to lack of light focusing.

This work was sponsored by NASA as technology validation for a miniature anemometer to be used in wind and dust particle studies on Mars and other planets. Thus the goal is an illumination bench that produces a small (tens of microns across) sensing volume a few centimeters away from the bench. To combine good focusing, small size, and rugged construction that are important for planetary missions, we pursued the use of a micromachined Si bench as a means of aligning all optical elements, including a flip-chip mounted semiconductor laser die.

The scope of this project was limited to building and testing the illumination bench. A complete miniature device should include the detector and detector optics located on the same bench. We chose to use red lasers for the ease of alignment. While low power of such lasers may be sufficient for some applications, more powerful near infrared laser dice should be used to detect small particles.

DEVICE LAYOUT, FABRICATION, AND ALIGNMENT

A photograph of the illuminator is presented in Figure 2. The device is approximately 18 mm long and 6 mm wide. The size can be further reduced without significant redesign. The light emitted from the facets of the die is collected by two GRIN lenses (G1, G2),

sent to two opposing mirrors (M1 and M2) and is focused at the intersection point approximately 23 mm above the bench.

To facilitate easy alignment, we used two independent Si substrates: the mirrors are mounted on the lower substrate, while the laser die and GRIN lenses are mounted on the top bench. The mirrors were affixed with epoxy in shallow recesses etched in the bottom substrate for the part registration. The top bench has a Au/Sn solder bump⁵ for the laser die attachment and etched V-grooves⁶ for the GRIN lens axial positioning. While the V-groove depth and the bump height were matched to provide the correct vertical registration, the horizontal alignment was achieved by attaching the laser die

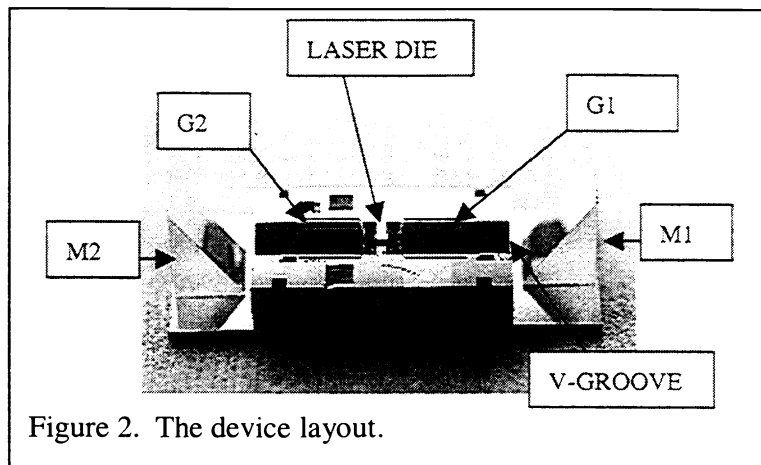


Figure 2. The device layout.

with a precision flip-chip bonder (Research Devices MG-8). We used alignment marks defined lithographically simultaneously (on the same layer) with the V-groove outline. The bonder provides lateral placement accuracy of $\pm 1.5 \mu\text{m}$. The recommended temperature for the die attachment is 300-350 °C (see Ref. 5). We have used the tool temperature of 370 °C to which we arrived by experimentation since the bonder provides no direct measurement of the solder bump temperature.

The uncoated laser dice used in this project were provided by SDL, Inc. As found through testing, they lase at 660 nm at room temperature and emit single mode in a wide range of currents. This range for the die used in the reported device is approximately 40-75 mA (it is somewhat die-specific). The use of uncoated dice will probably lead to low reliability of this device. However, obtaining custom coated dice would be prohibitively expensive for this project.

The device was mounted on a rotation stage so that the top bench with the die and GRIN lenses could be rotated versus the bottom substrate with the mirrors to effect the beam crossing. The GRIN lenses were placed in V-grooves and moved axially using micropositioners. We monitored the beam intersection area during alignment by projecting it onto a CCD camera focal plane through a microscope objective. Once the best alignment was achieved, we 'tacked' the GRIN lenses to the upper bench and the upper bench to the lower substrate using UV-curable epoxy.

TEST RESULTS AND DISCUSSION

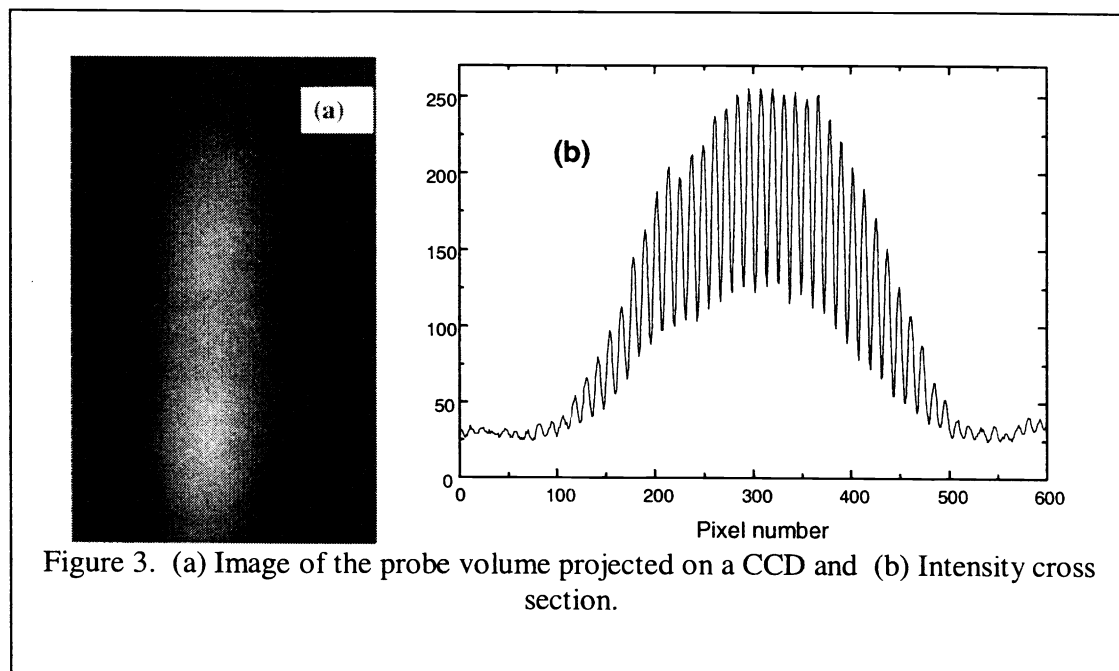
In order to validate the design and the alignment procedure we have performed two tests. Firstly, we have imaged the probe volume of the illuminator and analyzed the cross section. Secondly, we have performed the velocity measurement calibration. The

calibration data is consistent with predictions based on calculations using design parameters.

Probe volume cross section

To analyze the probe volume, we imaged it through a microscope objective with N.A. of 0.85, large enough to collect all the light. The image was projected onto the focal plane of a CCD camera and was grabbed using a National Instruments image board. The image is presented in Figure 3(a) and the fringe profile is shown in Figure 3b.

The expected cross section of the beam waist is an oblong shape determined by the angle θ and by the laser beam divergence in the vertical and horizontal planes. The evaluation of the expected probe volume cross section size started with measuring the divergence of the laser beam ($38^\circ \times 13^\circ$ full width @ $1/e$ power). Then the beam convergence after the GRIN lens was computed using its angular magnification of $1/17$. Finally, the beam waist size along the wide and narrow dimensions was calculated using expressions for Gaussian beams⁷. Taking into account the angle between the beams ($\theta=20^\circ$), the diffraction limited probe volume cross section at the beam waste was estimated at $6 \times 18 \mu\text{m}$.



The probe volume cross section is approximately 25 fringes wide at $1/e$ level, as can be seen in Figure 3b. Since the calculated fringe spacing is $0.95 \mu\text{m}$, that translates into the narrow dimension of $24 \mu\text{m}$, much larger than the diffraction limited value. Possible contributions to this discrepancy include non-optimal focusing and image distortions due to the GRIN lens quality. Using Figure 3a, the aspect ratio of the probe volume cross section is approximately 4:1, somewhat larger than the 3:1 ratio predicted above. We believe this is due to slight misalignment of the two laser beams. Such misalignment

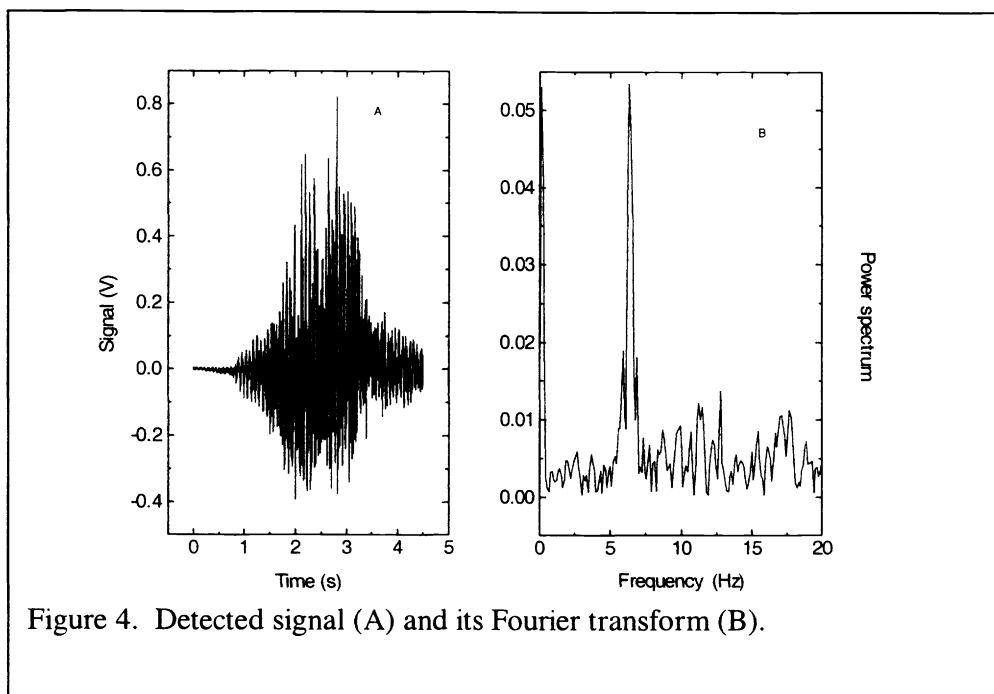


Figure 4. Detected signal (A) and its Fourier transform (B).

may as well explain the 1:1 ratio of the fringe depth to the fringe minima whereas full extinction at the minima were expected.

Velocity calibration

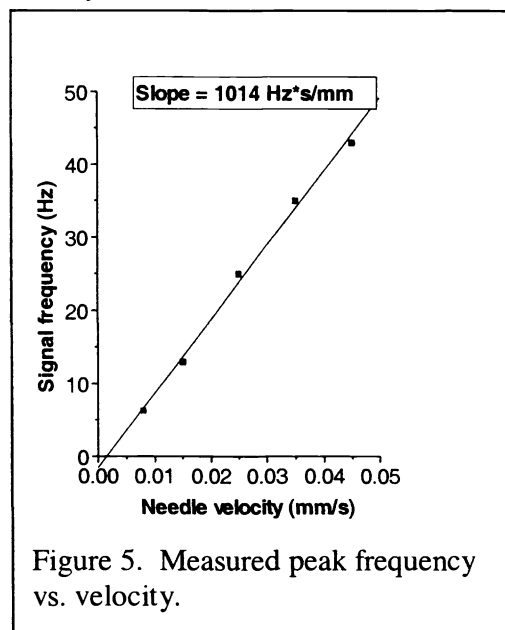


Figure 5. Measured peak frequency vs. velocity.

The velocity measurement was calibrated using a motorized translation stage driven by the Newport 850F actuator coupled to the Newport PMC-200 controller. The end of a $0.6 \mu\text{m}$ diameter probe was dragged through the active area using aforementioned stage. The scattered light was focused through a lens onto a Si detector. The detector was connected to a current amplifier input; the output was connected to a PC using a National Instruments Lab-PC signal processing board.

The spectrum of the measured signal was plotted and analyzed as shown in Figure 4. For speeds below 0.05 mm/s the Fourier transform of the signal yielded a distinct single peak as shown in Figure 4. At velocities above 0.05 mm/s very strong

parasitic modes in the frequency region of interest appeared and obscured useful information. We found through additional experimentation that these are the vibrational modes of the needle and the needle holder that are excited when the stage is running. Therefore only data points for velocities below 0.05 mm/s were used to obtain velocity calibration. In Figure 5 we have plotted the frequency of the peak in the signal spectrum vs. the stage velocity. The linear fit of experimental data plotted as the peak frequency

vs. velocity yielded a slope of 1014 Hz/(mm/s). The expected slope of 1036 Hz/(mm/s) was calculated using Equation 2 with the laser wavelength of 0.66 μm and the angle θ of 20°. This is in close agreement with the measured value.

CONCLUSIONS

We have demonstrated a miniature illuminator for Laser Doppler velocimeter on micromachined optical bench utilizing a novel optical scheme. The device calibration yields the slope of the signal frequency vs. velocity dependence close to the theoretical prediction. The analysis of the probe volume cross section suggests non-optimal focusing and slight beam misalignment.

ACKNOWLEDGMENTS

The research described in this paper was performed by the Center for Space Microelectronics Technology, Jet Propulsion Laboratory, California Institute of Technology, and was sponsored by the Directors research and Development Fund.

REFERENCES

1. F. Durst, R. Muller, and A. Naqwi. 'Semiconductor laser Doppler anemometer for applications in aerodynamic research', *AIAA Journal*, **30** (4) pp. 1033-1038, 1992
2. J. Seki, 'Fiber-optic laser-Doppler anemometer microscope developed for the measurement of microvascular red cell velocity', *Microvascular Research*, **40**, pp. 302-316, 1990
3. H.W. Jentik, J.A. J. van Beurden, M.A. Heisdingen, F.F. de Mul, H. E. Suiches, J. G. Aarnoduse, and J. Greeve, 'A compact differential laser Doppler velocimeter using a semiconductor laser', *J. Phys. E*, **20** pp.1281-1283, 1987
4. T. Ito, R. Sawada, and E. Higurashi. 'Integrated microlaser Doppler velocimeter', *J. Lightwave Technol.* **17** (1) pp. 30-34, 1999
5. J.H. Lau, *Flip Chip Technologies*, McGraw Hill, New York, 1996
6. K. Petersen, "Silicon as micromechanical material", *Proc. IEEE* **70** (5) pp. 420-457, 1982
7. P.W. Milonni and J.H. Eberly, *Lasers*, John Wiley & Sons, New York, 1988